

Socially Aware Robot Crowd Navigation with Interaction Graphs and Human Trajectory Prediction

Shuijing Liu*, Peixin Chang*, Zhe Huang, Neeloy Chakraborty, Weihang Liang, Junyi Geng, and Katherine Driggs-Campbell

Abstract—We study the problem of safe and socially aware robot navigation in dense and interactive human crowds. Previous works use simplified methods to model the personal spaces of pedestrians and ignore the social compliance of the robot behaviors. In this paper, we provide a more accurate representation of personal zones of walking pedestrians with their future trajectories. The predicted personal zones are incorporated into a reinforcement learning framework to prevent the robot from intruding into the personal zones. To learn socially aware navigation policies, we propose a novel recurrent graph neural network with attention mechanisms to capture the interactions among agents through space and time. We demonstrate that our method enables the robot to achieve good navigation performance and non-invasiveness in challenging crowd navigation scenarios. We successfully transfer the policy learned in the simulator to a real-world TurtleBot 2i.

I. INTRODUCTION

As robots are increasingly used in human-centric environments, social navigation in dynamic human crowds is an important yet challenging problem. In public spaces, people have clear norms about personal spaces that others should avoid breaking into [1], [2]. A robot that intrudes into people’s personal space can make them feel uncomfortable and may even result in accidents [3]. To navigate in a safe and socially aware manner, the robot must reason about the interactions in the crowd and avoid intrusions into the personal spaces of its surrounding pedestrians.

Robot navigation in dynamic and crowded environments has received much attention for many years [4]–[8]. Previous works have utilized heuristic methods and learning-based methods to determine the robot’s optimal action [6], [8]–[13]. These methods define the humans’ personal zones as *simplistic circles* centered at the humans with fixed radii, which represent the non-traversable regions for the robot, as shown in Fig. 1a. However, the circular personal zones ignore the past motions and future intentions of walking humans. In addition, these methods only consider the interactions between the robot and humans, while ignoring the human-human interactions. As a result, the navigation performance and the social awareness of the robot deteriorate in more challenging scenarios where the crowd is denser and the behaviors of pedestrians are more complicated.

* denotes equal contribution.

S. Liu, P. Chang, Z. Huang, W. Liang, N. Chakraborty and K. Driggs-Campbell are with the Department of Electrical and Computer Engineering at the University of Illinois at Urbana-Champaign. emails: {sliu105,pchang17,zheh4,neeloy2,weihang2,krcd}@illinois.edu

J. Geng is with the Robotics Institute at Carnegie Mellon University. email: junyigen@andrew.cmu.edu

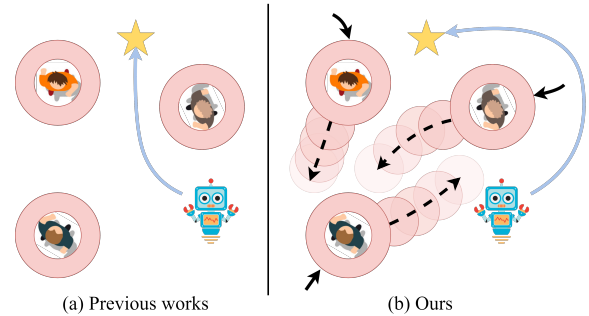


Fig. 1: The simplistic personal zones and our prediction-based personal zones. (a) A simplistic social zone of a walking pedestrian is a circle centered at the pedestrian’s position, which may result in unsafe or unsocial robot behaviors. (b) Our prediction-based social zone of a pedestrian is a set of circles centered at its future positions, which improves the performance and social awareness of the robot.

To incorporate future intentions of pedestrians into planning, trajectory-based crowd navigation methods first use trajectory predictors to predict other agents’ trajectories for one step. Then, the predicted trajectories are used to learn state transition probabilities and plan a feasible path for the robot [14]–[17]. However, these works do not utilize the predicted paths to improve the social awareness of the robot, since (1) the one-step predictions do not capture the long-term intent of each human, and (2) the planner does not penalize the robot if it intrudes into the predicted paths, which may still lead to impolite behaviors in Fig. 1a.

To address these problems, we create a learning framework for socially aware robot navigation in dense and interactive human crowds. As shown in Fig. 1b, we redefine the personal zones of walking humans as a set of circles centered at their future positions and approximate the personal zones with a pretrained pedestrian trajectory predictor. The *prediction-based personal zones* capture the interactions and future intentions of people in a crowd more accurately than the *simplistic circles*. To learn a robot policy, we then incorporate the predicted personal zones into a model-free reinforcement learning (RL) framework, which effectively prevents the robot from intruding into humans’ personal zones.

We model the crowd navigation scenario as a spatio-temporal (st) interaction graph to capture the interactions among agents through both space and time. Then, we convert the st-interaction graph to a novel end-to-end neural network and train it with RL. We use multi-head attention to model the human-human and robot-human spatial interactions. The attention networks enable the robot to pay attention to the important interactions, which ensures its good performance when the number of humans increases and the st-interaction

graph becomes complex. With the predicted personal zones and the interaction graph neural network, the learned robot policy is proactive, resilient, and non-invasive while navigating through dense and interactive crowds.

The main contributions of this paper are as follows. (1) We redefine the personal zones for walking human crowds with their future motions. We propose a novel method to incorporate the predicted personal zones into a model-free RL framework for robot crowd navigation. (2) We propose a novel graph neural network that uses attention mechanism to effectively capture the spatial and temporal interactions among heterogeneous agents. (3) The experiments demonstrate that our method outperforms previous works in terms of navigation performance and social awareness.

This paper is organized as follows: We review previous related works in Section II. We formalize the problem and propose our network architecture in Section III. Experiments and results in simulation and in the real world are discussed in Section IV and Section V, respectively. Finally, we conclude the paper in Section VI.

II. RELATED WORKS

A. Crowd navigation with simplistic personal zones

Proxemic distances define circular areas in which a person feels comfortable interacting with others [1], [3]. In Fig 1a, many crowd navigation methods use proxemic circles to represent regions that a robot is not supposed to traverse [2], [18], [19]. Heuristic methods such as optimal reciprocal collision avoidance (ORCA) and social force (SF) use one-step interaction rules to model the interactions with other agents and plan paths for the robot [6], [9], [10]. Another line of work, named Deep V-Learning, first uses supervised learning and then RL to learn a value function for path planning based on known state transitions of all agents [8], [11], [12], [20]. To remove assumptions on state transitions, decentralized structural-RNN (DS-RNN) uses model-free RL to train the robot policy from scratch with RL [13]. To model the interactions between the robot and humans, these RL-based methods use long short-term memory (LSTM) encoders, attention mechanisms, and spatio-temporal graphs.

However, all of the above methods only consider sparse or simple human crowds. In dense crowds where the pedestrians interact with each other more frequently, the safety and politeness of the robot degrade significantly because of the following two reasons. (1) The shapes of their personal zones distort and become difficult to approximate with geometric methods. (2) Compared with sparse crowds, interactions among humans have a larger effect on robot decision-making but are not explicitly modeled.

B. Crowd navigation with trajectory predictions

The pedestrian trajectory prediction community has made significant progress in modeling interactions among human crowds to predict their future motions [21]–[24]. In an effort to improve social navigation, trajectory-based methods first predict the future positions of humans for one timestep to learn the state transition probabilities of all agents. Then,

the state transition probabilities are used to search for the best robot path in d -step planning [14]–[17]. However, this pipeline does not improve the social awareness of the robot for the following two reasons: (1) The cost functions of the planners do not depend on the predicted human trajectories. Thus, it is difficult to prevent the robot from intruding into the intended paths of humans. (2) In each planning step, the predictors only predict the future human motions for one timestep, which only captures the instantaneous velocities and directions of pedestrians yet ignores their long-term intent. As a result, the robot is only able to perform reactive collision avoidance with humans. The politeness of the robot does not improve significantly compared with other methods without predictions. Although some other works attempt to predict the long-term goals of pedestrians to aid planning, the set of all possible goals is finite and small, which limits the generalization of these methods [25], [26].

To address the above problems, we incorporate predictions for several timesteps into the model-free RL framework so that the robot policy takes the long-term intents of pedestrians into account. In addition, the goals of pedestrians can be any position in a continuous two-dimensional space, which enables our method to generalize to more complex pedestrian behaviors.

C. Attention mechanism for crowd interactions

Attention mechanisms have been widely applied in sequence-based tasks such as trajectory prediction, crowd navigation, and machine translation [8], [13], [23], [27]–[29]. Vaswani et al. propose a self-attention mechanism that achieves state-of-the-art performance in machine translation [30]. For each word in a sentence, self-attention computes attention scores for all other words, which better captures the relationships among the words in a long sequence than an RNN that processes the words sequentially. Similarly, in trajectory prediction, attention networks value the importance of each pairwise interaction among participants, which improves the predictions of their future trajectories [8], [23], [27]. In crowd navigation of robots and vehicles, previous works have used attention networks to score the importance of each human neighbor to the controlled agent [8], [13], [31]. Compared with these works that ignore the interactions between humans, our attention networks capture the interactions among all observed agents and thus generalize better in dense and highly interactive human crowds.

III. METHODOLOGY

In this section, we first formulate the crowd navigation as an RL problem and introduce the social reward function. Then, we present our approach to model the crowd navigation scenario as a spatio-temporal interaction graph, which leads to the derivation of our network architecture.

A. Preliminaries

1) *MDP formulation*: Consider a robot navigating and interacting with humans in a 2D Euclidean space. We model

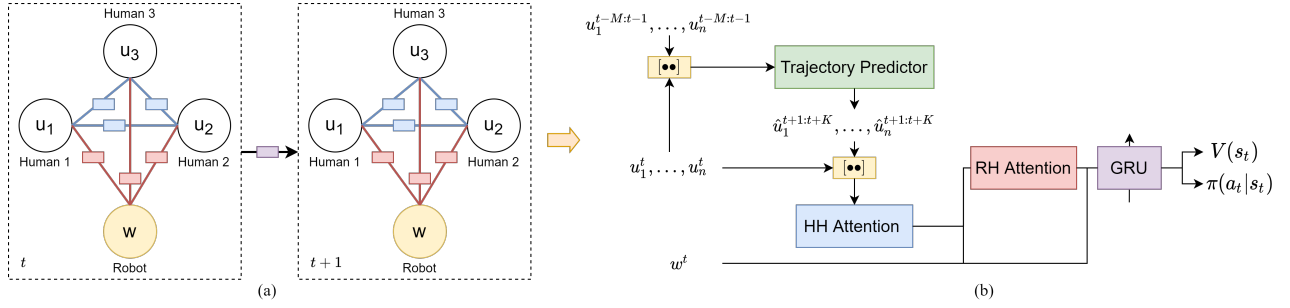


Fig. 2: **The spatial-temporal interaction graph and the network architecture.** (a) Graph representation of crowd navigation. The robot node is denoted by w and the i -th human node is denoted by u_i . HH edges and HH interaction functions are in blue, while RH edges and RH interaction functions are in red. Temporal function that connects the graphs at adjacent timesteps is in purple. (b) Our network. A trajectory predictor is used to predict personal zones. Two attention mechanisms are used to model the human-human interactions and robot-human interactions. We use a GRU as the temporal function.

the scenario as a Markov Decision Process (MDP), defined by the tuple $\langle S, \mathcal{A}, \mathcal{P}, R, \gamma, S_0 \rangle$. Let w^t be the robot state which consists of the robot's position (p_x, p_y) , goal position (g_x, g_y) , maximum speed v_{max} , heading angle θ , and radius of the robot base ρ . Let u_i^t be the current state of the i -th human at time t , which consists of the human's position (p_x^i, p_y^i) . Then, the K future and the M previous positions of the i -th human are denoted as $\hat{u}_i^{t+1:t+K}$ and $u_i^{t-M:t-1}$, respectively. We define the state $s_t \in \mathcal{S}$ of the MDP to be $s_t = [w^t, u_1^t, \hat{u}_1^{t+1:t+K}, \dots, u_n^t, \hat{u}_n^{t+1:t+K}]$ if a total number of n humans are observed at the timestep t , where n may change within a range in different timesteps.

In each episode, the robot begins at an initial state $s_0 \in S_0$. According to its policy $\pi(a_t|s_t)$, the robot takes an action $a_t \in \mathcal{A}$ at each timestep t . In return, the robot receives a reward r_t and transits to the next state s_{t+1} according to an unknown state transition $\mathcal{P}(\cdot|s_t, a_t)$. Meanwhile, all other humans also take actions according to their policies and move to the next states with unknown state transition probabilities. The process continues until the robot reaches its goal, t exceeds the maximum episode length T , or the robot collides with any humans.

2) *Reward function:* To discourage the robot from intruding into the predicted personal zones of humans and to increase its social awareness, we use a social reward r_{social} to penalize such intrusions:

$$\begin{aligned} r_{social}^i(s_t) &= \min_{k=1, \dots, K} \left(\mathbb{1}_i^{t+k} \frac{r_c}{2^k} \right) \\ r_{social}(s_t) &= \min_{i=1, \dots, n} r_{social}^i(s_t) \end{aligned} \quad (1)$$

where $\mathbb{1}_i^{t+k}$ indicates whether the robot collides with the predicted position of the human i at time $t+k$ and $r_c = -20$ is the penalty for collision. We assign different weights to the intrusions at different prediction timesteps, and thus the robot gets less penalty if it intrudes into the predicted social zone further in the future.

In addition, we add a potential-based reward $r_{pot} = 2(-d_{goal}^t + d_{goal}^{t-1})$ to guide the robot to approach the goal, where d_{goal}^t is the L_2 distance between the robot position and goal position at time t . Let S_{goal} be the set of goal states, where the robot successfully reaches the goal, and S_{fail} be the set of failure states, where the robot collides with any

human. Then, the whole reward function is defined as

$$r(s_t, a_t) = \begin{cases} 10, & \text{if } s_t \in S_{goal} \\ r_c, & \text{if } s_t \in S_{fail} \\ r_{pot}(s_t) + r_{social}(s_t), & \text{otherwise.} \end{cases} \quad (2)$$

Intuitively, the robot gets a high reward when it approaches the goal and avoids intruding into the current and future positions of all humans.

Let $\gamma \in (0, 1]$ be the discount factor. Then, $R_t = \sum_{k=0}^{\infty} \gamma^k r_{t+k}$ is the total accumulated return from timestep t . The goal of the agent is to maximize the expected return, $R_t = \mathbb{E}[\sum_{i=t}^T \gamma^{i-t} r_i]$, where γ is a discount factor. The value function $V^\pi(s)$ is defined as the expected return starting from s , and successively following policy π .

B. Spatio-Temporal Interaction Graph

We formulate the crowd navigation scenario as a spatio-temporal (st) interaction graph. As shown in Fig. 2a, at each timestep t , our st-interaction graph $\mathcal{G}_t = (\mathcal{V}_t, \mathcal{E}_t)$ consists of a set of nodes \mathcal{V}_t and a set of edges \mathcal{E}_t . The nodes in the st interaction graph represent the visible agents. The edges connect two different visible agents and represent the spatial interactions between the agents at the same timestep. The invisible humans that fall out of the robot's field of view and their corresponding edges are not included in the graph \mathcal{G}_t , since the robot cannot predict or integrate their motions in planning. Since we have control of the robot but not the humans, the human-human interactions and the robot-human interactions have different effects on the robot decision-making. Thus, we divide the set of edges \mathcal{E}_t into the human-human (HH) edges that connect two humans and the robot-human (RH) edges that connect the robot and a human, as shown in Fig. 2a. The two types of edges allow us to factorize the spatial interactions into HH interaction function and RH interaction function. In Fig. 2a, the HH and RH functions are denoted by the blue boxes and red boxes respectively and have parameters that need to be learned. Compared with the previous works that ignore HH edges [6], [8], [10], [13], our method considers the pair-wise interactions among all visible agents and thus scales better in dense and highly interactive crowds.

Since the movements of all agents cause the visibility of each human to change dynamically, the set of nodes \mathcal{V}_t and

edges \mathcal{E}_t and the parameters of the interaction functions may change correspondingly. To this end, we integrate the temporal correlations of the graph \mathcal{G}_t at different timesteps using another function denoted by the purple box in Fig. 2a. The temporal function connects the graphs at adjacent timesteps, which overcomes the short-sightedness of reactive methods and enables long-term decision-making of the robot.

To reduce the number of parameters, the same type of edges share the same function parameters. This parameter sharing is important for the scalability of our st interaction graph because the number of parameters is kept constant with an increasing number of humans [32].

C. Network Architecture

As shown in Fig. 2b, we derive our network architecture from the st-interaction graph. In our network, a pretrained trajectory predictor predicts the personal zones of humans. We represent the HH and RH functions as feedforward networks with attention mechanisms, referred to as HH attn and RH attn respectively. We represent the temporal function as a gated recurrent unit (GRU). We use W and f to denote trainable weights and fully connected layers throughout this section.

1) *Trajectory predictor*: Since the robot has a limited field of view and the tracking of humans is imperfect, we use a Gumbel Social Transformer (GST), which provides unbiased modeling of partially detected humans, to predict the personal zones of humans [28]. As shown in Fig. 2b, the trajectory predictor takes the trajectories of observed humans from time $t - M$ to t as input and predicts their future trajectories from time $t + 1$ to $t + K$:

$$\hat{\mathbf{u}}_i^{t+1:t+K} = GST(\mathbf{u}_i^{t-M:t}), \quad i \in \{1, \dots, n\} \quad (3)$$

We concatenate the current states and the predicted future states of humans as one of the input observations of the robot policy network. To compute the intrusions in Eq. 1 for rewards, we add a circle centered at each predicted position to approximate personal zones as shown in Fig. 1b.

2) *Attention mechanisms*: The HH and RH attention functions are similar to the scaled dot-product attention in [30], which computes attention score using a query Q and a key K , and apply the normalized score to a value V .

$$\text{Attn}(Q, K, V) = \text{softmax}\left(\frac{QK^\top}{\sqrt{d}}\right)V \quad (4)$$

where d is the dimension of the queries and keys.

In HH attention, the current states and the predicted future states of humans are concatenated and passed through linear layers to obtain $Q_{HH}^t, K_{HH}^t, V_{HH}^t \in \mathbb{R}^{n \times d_{HH}}$, where d_{HH} is the attention size for the HH attention.

$$\begin{aligned} Q_{HH}^t &= [\mathbf{u}_1^{t:t+K}, \dots, \mathbf{u}_n^{t:t+K}]^\top W_{HH}^Q \\ K_{HH}^t &= [\mathbf{u}_1^{t:t+K}, \dots, \mathbf{u}_n^{t:t+K}]^\top W_{HH}^K \\ V_{HH}^t &= [\mathbf{u}_1^{t:t+K}, \dots, \mathbf{u}_n^{t:t+K}]^\top W_{HH}^V \end{aligned} \quad (5)$$

We obtain the human embeddings $v_{HH}^t \in \mathbb{R}^{n \times d_{HH}}$ using a multi-head scaled dot-product attention, and the number of attention heads is 8.

In RH attention, $K_{RH}^t \in \mathbb{R}^{1 \times d_{RH}}$ is the linear embedding of the robot states \mathbf{w}^t and $Q_{RH}^t, V_{RH}^t \in \mathbb{R}^{n \times d_{RH}}$ are linear embeddings of the weighted human features from HH attention v_{HH}^t .

$$Q_{RH}^t = v_{HH}^t W_{RH}^Q, \quad K_{RH}^t = \mathbf{w}^t W_{RH}^K, \quad V_{RH}^t = v_{HH}^t W_{RH}^V \quad (6)$$

We compute the attention score from Q_{RH}^t and K_{RH}^t as in Eq. 4, transpose the score, and apply the score to V_{RH}^t to obtain the twice weighted human features $v_{RH}^t \in \mathbb{R}^{1 \times d_{RH}}$ with a single head.

In HH and RH attention networks, we use binary masks that indicate the visibility of each human to prevent attention to invisible humans. Unlike DS-RNN that fills the invisible humans with dummy values [13], the masks provide unbiased gradients to the attention networks, which stabilizes and accelerates the training.

3) *GRU*: We embed the robot states \mathbf{w}^t with linear layers f_R to obtain v_R^t , which are concatenated with the twice weighted human features v_{RH}^t and fed into the GRU:

$$v_R^t = f_R(\mathbf{w}^t), \quad h^t = \text{GRU}(h^{t-1}, ([v_{RH}^t, v_R^t])) \quad (7)$$

where h^t is the hidden state of GRU at time t . Finally, the h^t is input to a fully connected layer to obtain the value $V(s_t)$ and the policy $\pi(a_t|s_t)$.

4) *Training*: We train the trajectory predictor with a dataset of human trajectories collected from our simulator. In RL training, we freeze the trainable parameters of the trajectory predictor and only run inference. We train trajectory predictor and RL policy separately because the two tasks have different objectives, resulting in unstable and less efficient joint training. We use Proximal Policy Optimization (PPO), a model-free policy gradient algorithm, for policy and value function learning [33]. To accelerate and stabilize training, we run 16 instances of the environment in parallel for collecting the robot's experiences. At each policy update, 30 steps of six episodes are used.

IV. SIMULATION EXPERIMENTS

In this section, we present our simulation environment, experiment setup, and experimental results in simulation.

A. Simulation environment

Our 2D environment simulates a scenario where a robot navigates through a dense crowd relying on a sensor with a limited range, as shown in Fig. 3. Our simulation captures the more realistic crowd navigation scenarios than the simulations in the previous works in two aspects [8], [13]. First, our robot sensor has a limited range of $5m$, while the previous works unrealistically assume that the robot has an infinite detection range. Second, the maximum number of humans can reach up to 20, leading to a denser and more interactive human crowd.

In our simulations, the robot's sensor range is set to $5m$ and remains unchanged. In each episode, the starting and goal positions of the robot and the humans are randomly placed on the 2D plane. To simulate a continuous human

TABLE I: Navigation results with randomized humans

Method	SR \uparrow	NT \downarrow	PL \downarrow	ITR \downarrow	SD \uparrow
ORCA	69.0	14.77	17.67	19.61	0.38
SF	29.0	20.28	15.93	17.68	0.37
DS-RNN	64.0	16.31	19.63	23.91	0.34
Ours (No pred, HH attn)	67.0	16.82	20.19	16.13	0.37
Ours (GST, no HH attn)	77.0	12.96	18.43	8.24	0.40
Ours (Const vel, HH attn)	87.0	14.03	20.14	7.00	0.42
Ours (GST, HH attn)	89.0	15.03	21.31	4.18	0.44
Ours (Oracle, HH attn)	90.0	16.03	22.82	1.70	0.47

flow, humans will move to new random goals immediately after they arrive at their goal positions. All humans are controlled by ORCA and react only to other humans but not to the robot. This invisible setting prevents our model from learning an extremely aggressive policy in which the robot forces all humans to yield while achieving a high reward. We use holonomic kinematics for each agent, whose action at time t consists of the desired velocity along the x and y axis, $a_t = [v_x, v_y]$. We assume that all agents can achieve the desired velocities immediately, and they will keep moving with these velocities for the next Δt seconds. We define the update rule for an agent’s position p_x, p_y as follows:

$$\begin{aligned} p_x[t+1] &= p_x[t] + v_x[t]\Delta t \\ p_y[t+1] &= p_y[t] + v_y[t]\Delta t \end{aligned} \quad (8)$$

We use two simulation environments for experiments. The first environment simulates more complex real-world crowds with the following randomizations. First, all humans occasionally change their goal positions within an episode. Second, each human has randomly assigned maximum speed v_{max} and the radius of the robot base ρ . The second environment has no such randomized human behaviors. The crowds in both environments are dense and interactive, while the randomizations in the first environment pose extra challenges for prediction and decision making.

B. Experiment setup

1) *Baselines and Ablation Models*: We compare the performance of our model with the representative methods for crowd navigation. We choose GST as the trajectory predictor and denote our method as (GST, HH attn). We choose ORCA [6] and SF [10] as the reactive-based baselines and DS-RNN [13] as the learning-based baseline¹. To show the benefits of considering human-human interactions in RL policy, we test the performance of an ablated model, denoted as (GST, no HH Attn), where the HH attention layer is replaced with several fully-connected layers.

To show the benefits of incorporating a trajectory predictor, we compare the performance of our model with three ablation models. The first model does not use a trajectory predictor (No pred, HH attn). The second model uses a simple trajectory predictor which predicts the future trajectories by the latest velocity of the agent (Const vel, HH attn). The final model is an oracle model which has the access to the true future trajectory of an agent (Oracle, HH attn).

¹Comparison to more baselines can be found in [13]

TABLE II: Navigation results without randomized humans

Method	SR \uparrow	NT \downarrow	PL \downarrow	ITR \downarrow	SD \uparrow
ORCA	78.0	15.87	18.53	26.04	0.36
SF	34.0	19.95	17.75	21.35	0.35
DS-RNN	67.0	20.06	25.42	13.31	0.37
Ours (No pred, HH attn)	82.0	19.15	22.82	14.87	0.37
Ours (GST, no HH attn)	82.0	14.21	19.35	7.22	0.40
Ours (Const vel, HH attn)	94.0	18.26	23.98	4.49	0.43
Ours (GST, HH attn)	94.0	17.64	22.51	3.06	0.43
Ours (Oracle, HH attn)	94.0	15.38	21.23	2.97	0.45

2) *Training and Evaluation*: For all RL-based methods, we use the same reward as defined in Eq. 2 and train them for 2×10^7 timesteps with a learning rate 4×10^{-5} . We test all methods with 500 random unseen test cases. Our metrics include navigation metrics and social metrics. The navigation metrics measure the quality of the navigation and include the percentage success rate (SR), average navigation time (NT) in seconds, and path length (PL) in meters of the successful episodes. The social metrics measure the social awareness of the agent, which include intrusion time ratio (ITR) and social distance during intrusions (SD) in meters. The intrusion time ratio per episode is defined as c/C , where c is the number of timesteps that the robot is in any human’s ground truth social zone and C is the length of that episode. The ITR is the average ratio of all testing episodes. We define SD as the average distance between the robot and its closest human when an intrusion occurs. To ensure a fair comparison, all intrusions are calculated by ground truth future positions of humans.

C. Results

1) *Navigation performance*: The results of robot navigation in two simulation environments are shown in Table I and Table II. In both tables, our method (GST, HH attn) outperforms the ORCA, SF, DS-RNN, and the ablated model (GST, no HH attn) by a large margin in terms of success rate. Fig 3a, b, and d provide an example episode where (GST, HH attn) succeeds but ORCA and DS-RNN end up with collisions. Since the above four baselines and ablation only model RH interactions but ignore HH interactions, the HH attention and our graph network contribute to performance gain. These results suggest that the human-human interactions are essential for dense crowd navigation and are successfully captured by our HH attention mechanism.

To analyze the effects of prediction-based social zones, in both tables, we observe that the methods with predicted social zones (last four rows) generally have higher success rates than those without predicted social zones (first four rows). From the values of (No pred, HH attn), (Const vel, HH attn), and (GST, HH attn), we see that the trajectory predictors improve the success rate by around 20% and 12% in the scenarios with and without randomized human behaviors. Thus, the use of trajectory predictor for social zone approximation enables long-sighted robot decision making and thus also improves safety, as shown in Fig 3c and d. From Table I, in the randomized scenario, the trajectory

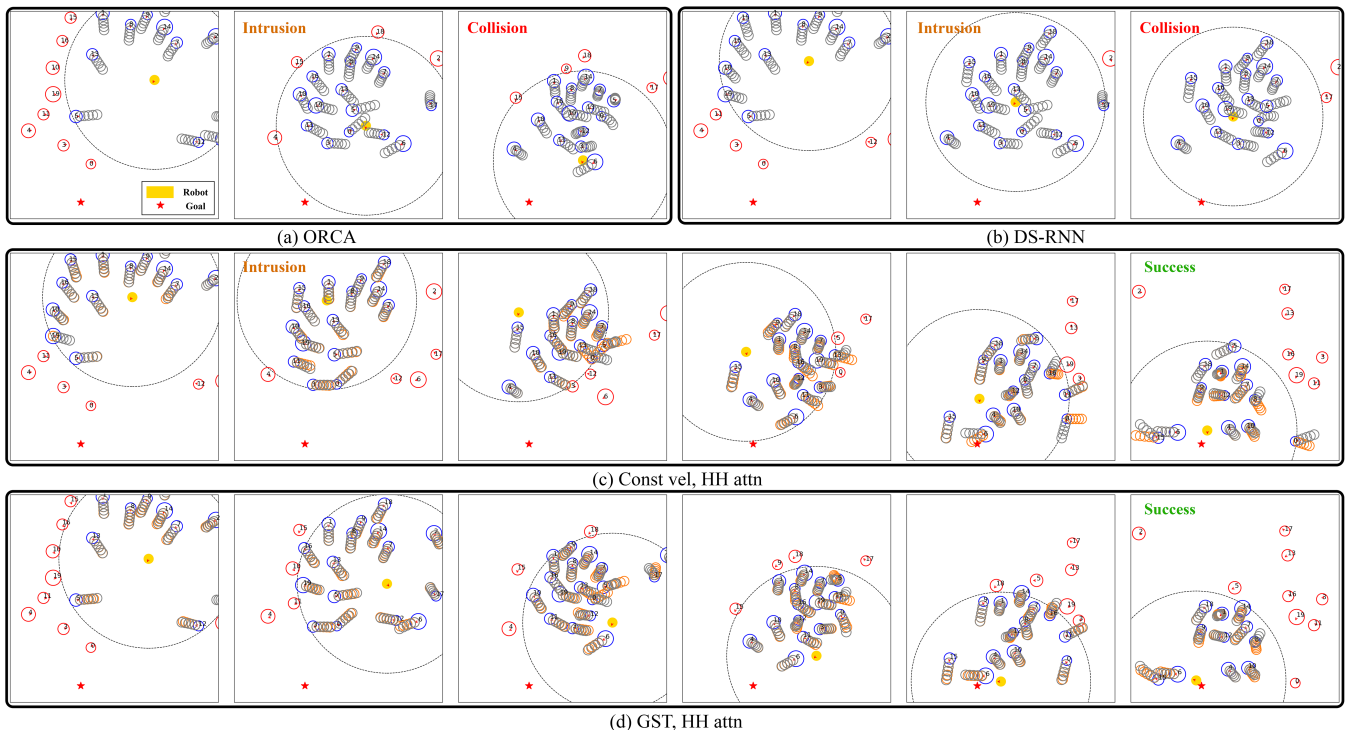


Fig. 3: Comparison of different methods in the same testing episode with randomized humans. The orientation of an agent is indicated by a red arrow, the robot is the yellow disk, and the robot’s goal is the red star. We outline the borders of the robot sensor range with dashed lines. Represented as empty circles, the humans in the robot’s field of view are blue and those outside are red. The ground truth future trajectories and personal zones are in gray and are only used to visualize intrusions, and the predicted trajectories are in orange. More qualitative results can be found in the video attachment.

predictors provide a larger performance gain since the crowd behaviors are more complicated and thus are more difficult to predict implicitly. In both scenarios, the navigation time and path length of (GST, HH attn) are not the shortest but closest to the oracle, followed by (Const vel, HH attn). The longer NT and PL is caused by our reward function that penalizes the robot to take short yet impolite paths. This trend also indicates that a better predictor leads to a better policy.

However, we also notice that in both scenarios, compared with constant velocity predictor, GST predictor only improves the success rate with small margins. The reason is that the humans in our simulator are controlled by ORCA, which prefers linear motion if no other agents are nearby. Thus, the prediction performance of GST on ORCA humans is only marginally better than the constant velocity model.

2) *Social awareness*: From the last three rows of Table I and Table II, we observe that compared with the baselines without predictions, the models aided by the trajectory predictors have significantly lower intrusion time ratio and higher social distance during intrusions. Among the models with predictors, our method (GST, HH attn) is the closest to the oracle in terms of intrusion time ratio and social distance and therefore, the robot is the least invasive and most polite. For example, the robot in Fig 3d always keeps a good social distance from the personal zones of all humans, while it occasionally intrudes the personal zones in Fig 3c. In contrast, without predicted personal zones, the robots in Fig 3a and b are notably more aggressive and impolite. These results indicate that the proposed prediction-based personal zones accurately capture the personal space of walking pedestrians.



Fig. 4: The setup of the real world experiment.

Moreover, better trajectory predictors can provide the robot policy with more accurate approximations of the personal zones and the reward function.

V. REAL-WORLD EXPERIMENTS

To show the effectiveness of our method on real physical robots, we deploy the model trained in the simulator to a TurtleBot 2i mobile platform shown in Fig. 4. We use an Intel RealSense tracking camera T265 to obtain the position and orientation of the robot. The human positions are estimated from 2D range data generated by an RPLIDAR-A3 laser scanner. We use DR-SPAAM, a 2D LIDAR person detector, to estimate the positions of humans and a Kalman Filter to track them [34], [35]. We run the above perception algorithms and our decision-making model on a remote host computer. Video demonstrations are available in the video attachment, where the robot keeps a safe distance from humans in various scenarios and successfully reaches the goals.

VI. CONCLUSION AND FUTURE WORK

We propose a novel framework that incorporates trajectory prediction and spatial-temporal reasoning for socially-aware

crowd navigation. We redefine the personal zones of the walking humans with their long-term future trajectories, which are incorporated into an RL learning framework to prevent the intrusions of the robot. We capture the spatial interactions in the crowd with self-attention mechanisms and propose a novel graph neural network to learn navigation policies. The experiments show that our method outperforms various baselines in partially-observed dense crowds and show promising results in the real world. Possible directions to explore in future work include (1) using datasets collected from real pedestrians to train our method, and (2) performing user studies to evaluate the social awareness of our model.

Acknowledgements: We thank Tianchen Ji for feedback on paper drafts.

REFERENCES

- [1] J. K. Burgoon and S. B. Jones, "Toward a theory of personal space expectations and their violations," *Human Communication Research*, vol. 2, no. 2, pp. 131–146, 1976.
- [2] A. Bera, T. Randhavane, R. Prinja, and D. Manocha, "Sociosense: Robot navigation amongst pedestrians with social and psychological constraints," in *IEEE/RSJ International Conference on Intelligent Robots and Systems (IROS)*, 2017, pp. 7018–7025.
- [3] L. Takayama and C. Pantofaru, "Influences on proxemic behaviors in human-robot interaction," in *IEEE/RSJ International Conference on Intelligent Robots and Systems (IROS)*, 2009, pp. 5495–5502.
- [4] D. Fox, W. Burgard, and S. Thrun, "The dynamic window approach to collision avoidance," *IEEE Robotics and Automation Magazine*, vol. 4, no. 1, pp. 23–33, 1997.
- [5] T. Kruse, A. K. Pandey, R. Alami, and A. Kirsch, "Human-aware robot navigation: A survey," *Robotics and Autonomous Systems*, vol. 61, no. 12, pp. 1726–1743, 2013.
- [6] J. Van Den Berg, S. J. Guy, M. Lin, and D. Manocha, "Reciprocal n-body collision avoidance," in *Robotics research*. Springer, 2011, pp. 3–19.
- [7] P. Trautman, J. Ma, R. M. Murray, and A. Krause, "Robot navigation in dense human crowds: Statistical models and experimental studies of human-robot cooperation," *The International Journal of Robotics Research*, vol. 34, no. 3, pp. 335–356, 2015.
- [8] C. Chen, Y. Liu, S. Kreiss, and A. Alahi, "Crowd-robot interaction: Crowd-aware robot navigation with attention-based deep reinforcement learning," in *IEEE International Conference on Robotics and Automation (ICRA)*, 2019, pp. 6015–6022.
- [9] J. Van Den Berg, M. Lin, and D. Manocha, "Reciprocal velocity obstacles for real-time multi-agent navigation," in *IEEE International Conference on Robotics and Automation (ICRA)*, 2008, pp. 1928–1935.
- [10] D. Helbing and P. Molnar, "Social force model for pedestrian dynamics," *Physical review E*, vol. 51, no. 5, p. 4282, 1995.
- [11] Y. F. Chen, M. Liu, M. Everett, and J. P. How, "Decentralized non-communicating multiagent collision avoidance with deep reinforcement learning," in *IEEE International Conference on Robotics and Automation (ICRA)*, 2017, pp. 285–292.
- [12] M. Everett, Y. F. Chen, and J. P. How, "Motion planning among dynamic, decision-making agents with deep reinforcement learning," in *IEEE/RSJ International Conference on Intelligent Robots and Systems (IROS)*, 2018, pp. 3052–3059.
- [13] S. Liu, P. Chang, W. Liang, N. Chakraborty, and K. Driggs-Campbell, "Decentralized structural-rnn for robot crowd navigation with deep reinforcement learning," in *IEEE International Conference on Robotics and Automation (ICRA)*, 2021, pp. 3517–3524.
- [14] C. Chen, S. Hu, P. Nikdel, G. Mori, and M. Savva, "Relational graph learning for crowd navigation," in *IEEE/RSJ International Conference on Intelligent Robots and Systems (IROS)*, 2020, pp. 10007 – 10013.
- [15] S. Eiffert, H. Kong, N. Pirmarzdashii, and S. Sukkari, "Path planning in dynamic environments using generative rnns and monte carlo tree search," in *IEEE International Conference on Robotics and Automation (ICRA)*, 2020, pp. 10 263–10 269.
- [16] K. Li, M. Shan, K. Narula, S. Worrall, and E. Nebot, "Socially aware crowd navigation with multimodal pedestrian trajectory prediction for autonomous vehicles," in *IEEE International Conference on Intelligent Transportation Systems (ITSC)*, 2020, pp. 1–8.
- [17] A. J. Sathiamoorthy, J. Liang, U. Patel, T. Guan, R. Chandra, and D. Manocha, "Densecavoid: Real-time navigation in dense crowds using anticipatory behaviors," in *IEEE International Conference on Robotics and Automation (ICRA)*, 2020, pp. 11 345–11 352.
- [18] D. Vasquez, B. Okal, and K. O. Arras, "Inverse reinforcement learning algorithms and features for robot navigation in crowds: An experimental comparison," in *IEEE/RSJ International Conference on Intelligent Robots and Systems (IROS)*, 2014, pp. 1341–1346.
- [19] A. Bera, T. Randhavane, and D. Manocha, "The emotionally intelligent robot: Improving socially-aware human prediction in crowded environments," in *IEEE/CVF Conference on Computer Vision and Pattern Recognition (CVPR) Workshops*, 2019.
- [20] Y. Chen, C. Liu, B. E. Shi, and M. Liu, "Robot navigation in crowds by graph convolutional networks with attention learned from human gaze," *IEEE Robotics and Automation Letters*, vol. 5, no. 2, pp. 2754–2761, 2020.
- [21] A. Alahi, K. Goel, V. Ramanathan, A. Robicquet, L. Fei-Fei, and S. Savarese, "Social lstm: Human trajectory prediction in crowded spaces," in *IEEE/CVF Conference on Computer Vision and Pattern Recognition (CVPR)*, 2016, pp. 961–971.
- [22] A. Gupta, J. Johnson, L. Fei-Fei, S. Savarese, and A. Alahi, "Social gan: Socially acceptable trajectories with generative adversarial networks," in *IEEE/CVF Conference on Computer Vision and Pattern Recognition (CVPR)*, 2018, pp. 2255–2264.
- [23] A. Vemula, K. Muelling, and J. Oh, "Social attention: Modeling attention in human crowds," in *IEEE International Conference on Robotics and Automation (ICRA)*, 2018, pp. 1–7.
- [24] Y. Huang, H. Bi, Z. Li, T. Mao, and Z. Wang, "Stgat: Modeling spatial-temporal interactions for human trajectory prediction," in *IEEE International Conference on Computer Vision (ICCV)*, 2019.
- [25] K. D. Kalyal, G. D. Hager, and C.-M. Huang, "Intent-aware pedestrian prediction for adaptive crowd navigation," in *IEEE International Conference on Robotics and Automation (ICRA)*, 2020, pp. 3277–3283.
- [26] A. Vemula, K. Muelling, and J. Oh, "Modeling cooperative navigation in dense human crowds," in *IEEE International Conference on Robotics and Automation (ICRA)*, 2017, pp. 1685–1692.
- [27] P. Zhang, W. Ouyang, P. Zhang, J. Xue, and N. Zheng, "Sr-lstm: State refinement for lstm towards pedestrian trajectory prediction," in *IEEE/CVF Conference on Computer Vision and Pattern Recognition (CVPR)*, 2019, pp. 12 077–12 086.
- [28] Z. Huang, R. Li, K. Shin, and K. Driggs-Campbell, "Learning sparse interaction graphs of partially detected pedestrians for trajectory prediction," *IEEE Robotics and Automation Letters*, vol. 7, no. 2, pp. 1198–1205, 2022.
- [29] D. Bahdanau, K. Cho, and Y. Bengio, "Neural machine translation by jointly learning to align and translate," *arXiv preprint arXiv:1409.0473*, 2014.
- [30] A. Vaswani, N. Shazeer, N. Parmar, J. Uszkoreit, L. Jones, A. N. Gomez, Ł. Kaiser, and I. Polosukhin, "Attention is all you need," in *Advances in Neural Information Processing Systems (NeurIPS)*, 2017, pp. 5998–6008.
- [31] E. Leurent and J. Mercat, "Social attention for autonomous decision-making in dense traffic," in *Machine Learning for Autonomous Driving Workshop at Advances in Neural Information Processing Systems (NeurIPS)*, 2019.
- [32] A. Jain, A. R. Zamir, S. Savarese, and A. Saxena, "Structural-rnn: Deep learning on spatio-temporal graphs," in *IEEE/CVF Conference on Computer Vision and Pattern Recognition (CVPR)*, 2016, pp. 5308–5317.
- [33] J. Schulman, F. Wolski, P. Dhariwal, A. Radford, and O. Klimov, "Proximal policy optimization algorithms," *arXiv preprint arXiv:1707.06347*, 2017.
- [34] D. Jia, A. Hermans, and B. Leibe, "DR-SPAAM: A Spatial-Attention and Auto-regressive Model for Person Detection in 2D Range Data," in *IEEE/RSJ International Conference on Intelligent Robots and Systems (IROS)*, 2020, pp. 10 270–10 277.
- [35] mabhissharma, "Multi Object Tracking with Kalman-Filter," 2018. [Online]. Available: <https://github.com/mabhissharma/Multi-Object-Tracking-with-Kalman-Filter>